ELSEVIER

Available online at www.sciencedirect.com

SCIENCE DIRECT®

Journal of Solid State Chemistry 178 (2005) 1786–1798

JOURNAL OF SOLID STATE CHEMISTRY

www.elsevier.com/locate/jssc

Photophysics, photoelectrical properties and photoconductivity relaxation dynamics of quantum-sized bismuth(III) sulfide thin films

Biljana Pejova[a,*], Atanas Tanuševski[b], Ivan Grozdanov[a]

[a]Institute of Chemistry, Faculty of Natural Sciences and Mathematics, Sts. Cyril and Methodius University, P.O.B. 162, 1000 Skopje, Macedonia

[b]Institute of Physics, Faculty of Natural Sciences and Mathematics, Sts. Cyril and Methodius University, P.O.B. 162, 1000 Skopje, Macedonia

Received 17 January 2005; accepted 10 March 2005

Available online 18 April 2005

Abstract

Electrical and photoelectrical properties (including both the stationary photoresponse and the photocarriers' relaxation dynamics) of nanocrystalline semiconducting bismuth(III) sulfide thin films were investigated. The experimental design of photoelectrical properties was achieved by controlling the chemistry of the deposition process (varying the reagent concentration in the reaction system) and also by physical means (controlling the crystal dimensions by post-deposition annealing). The band gap energy of thin films characterized by most pronounced photoelectrical properties was calculated, on the basis of measured photoconductivity spectral response curves, by several approaches. All of the obtained values are in very good agreement with the corresponding ones obtained from optical spectroscopy data within the framework of parabolic approximation for dispersion relation. On the basis of measured temperature dependence of dark electrical resistivity of nanocrystalline bismuth(III) sulfide films, the thermal band gap energy and the ionization energy of the impurity level (of donor type) were calculated. The corresponding values are 1.50 and 0.42 eV. Dynamics of non-equilibrium charge carriers' relaxation processes was studied with the oscilloscopic method. By analysis of the photoconductivity decay kinetics data it is found that recombination of non-equilibrium charge carriers is carried out according to the linear mechanism. The calculated relaxation time of photoexcited charge carriers is 1.58 ms, the relaxation processes occurring via local trapping centers. Recombination processes occurring via a single-type trapping center can be described within the framework of the Schockley–Read model. The practically linear regime detected in the measured lux–ampere characteristics of the studied films ($\Delta\sigma \sim \Phi^{0.98}$) indicate as well a linear recombination mechanism of the photoexcited charge carriers.

© 2005 Published by Elsevier Inc.

Keywords: Bismuth(III) sulfide; Thin films; Semiconductors; Chemical deposition; Nano-crystals; Band gap energy; Quantum size effects; Electrical resistivity; Photoconductivity; Photoconductivity spectra; Relaxation time; Relaxation dynamics; Lux–ampere characteristics; Internal photoelectric effect

1. Introduction

In the last few years, the family of A^VB^{VI} semiconducting compounds with nanocrystalline structure has been a subject of investigation by many research groups. Their interesting optoelectronic properties make A^VB^{VI} thin film-based optoelectronic devices as one of the most promising developments in electronic applications [1–11]. Also, part of A^VB^{VI} semiconducting compounds, have received great attention since their band gap values lie close to the range of theoretically maximum attainable energy conversion efficiency [12]. As it has been firmly established in the last decade, the properties of nanostructured semiconducting materials deviate from those of single crystals or coarse-grained polycrystals with the same average chemical composition. So, semiconducting nanomaterials offer the possibility of materials engineering to enhance device characteristics. The study of the effect of crystal size on the physical and optical properties of semiconducting materials is thus a rather attractive topic [13,14].

*Corresponding author. Fax: +389 3 226 865.

E-mail address: biljana@iunona.pmf.ukim.edu.mk (B. Pejova).

0022-4596/$ - see front matter © 2005 Published by Elsevier Inc.

doi:10.1016/j.jssc.2005.03.017

In this study, the main emphasis of our research is put on the photoelectrical properties, especially the phenomenon of photoconductivity and also on the relaxation dynamics of photoexcited charge carriers in the case of quantum-sized bismuth(III) sulfide particles in thin film form which we have prepared using chemical deposition method. In our previous manuscript [15], we have presented the experimental details of synthesis of investigated material as thin film, its structural and optical properties and their evolution upon thermal treatments as well. The present paper is in fact a continuation of a series of our previous studies devoted to chemistry and physics of semiconducting materials in the form of thin films, especially those with nanocrystalline nature [16–25].

Bismuth(III) sulfide has the status of one of the earliest photoconducting materials known since 1920 [26]. For the first time, the phenomenon of photoconductivity of bismuth(III) sulfide, was reported by Case in 1917 [27], based on studies of mineral samples—bismuthinite or bismuth glance. There have been only a few reports in the literature regarding basic photoelectrical properties of Bi_2S_3 deposited in thin film form [2,6,28,29], but in none of these studies the deposited material was of nanocrystalline nature. Also, except in a recent paper by Kebbab and coworkers [2], no particular attention seems to be paid to the kinetics of photoconductivity decay. However, in Ref. [2], the investigated Bi_2S_3 thin films were deposited by the spray pyrolysis technique. As the properties of semiconducting materials deposited in thin film form are strongly dependent on the particular technique employed for their deposition, it is of certain interest to compare the properties of films of the same material, obtained by different deposition techniques.

Along with everything that has been previously said about this material, bismuth(III) sulfide, as a semiconductor with band gap energy in the visible solar energy spectrum, is a very useful material in the field of devices for solar energy conversion [2–14]. Besides purely practical and applicative aspects, the study of photoconductivity phenomenon in the case of bismuth(III) sulfide and of other materials as well, is an important topic also from a fundamental point of view. A profound analysis of this phenomenon is of essential importance for understanding the processes of charge-carriers generation, transport and therefore the features of electronic density of states in semiconductors in general [26].

2. Experimental details

2.1. Chemical deposition of bismuth(III) sulfide nanocrystals in thin film form

The thin films of bismuth(III) sulfide were deposited onto glass substrates using a method of chemical deposition. The experimental details of thin film deposition are presented in our previous manuscript [15]. Briefly, the thin films were grown at 60 °C in an acidic reaction system (with $pH = 2$) containing bismuth(III) nitrate and sodium thiosulfate as a sulfide ion precursor and as a complexing agent at the same time. To prevent the hydrolysis of Bi^{3+} ions, bismuth(III) nitrate was dissolved in a solution of nitric acid with $c(HNO_3) = 2\,mol/dm^3$. The proposed synthesis is based on controlled homogeneous precipitation reaction in liquid phase (i.e. in an acidic aqueous reaction system) which gives colloidal particles with narrow size distributions. The colloidal particles formed migrate to the used substrate and subsequently adsorb and aggregate onto its surface creating nanocrystalline thin films of bismuth(III) sulfide.

To improve the film adhesion, the substrates, prior to deposition process were dipped in a diluted solution of tin(II) chloride and then thermically treated at 200 °C. The small crystals of tin(II) oxide with stochastic distribution, which are formed onto the substrate surface as a result of its previous treatments, initiate heterogeneous nucleation during the deposition process [22]. Much more details regarding the overall chemistry of the deposition process may be found in our previous paper on this subject [15].

2.2. Characterization and basic structural properties of as-deposited and annealed bismuth(III) sulfide nanocrystals in thin film form

We have devoted our previous paper to a detailed study of structural and optical properties of as-deposited and thermally treated Bi_2S_3 nanocrystalline thin films [15]. For the purpose of this study, in this context we only briefly review the most relevant points. The as-deposited material (in thin film form and as bulk precipitate as well) is the pure orthorhombic modification of bismuth sulfide with stibnite type of structure (space group *Pbnm* (D_{2h}^{16}) [30]—the X-ray diffractograms were presented in details in our previous paper [15]). Upon annealing in air atmosphere up to 250 °C (for 10 min), no changes in chemical composition of deposited thin films were registered. Prolonging the annealing time to 3 h leads to incorporation of oxide and sulfate-phase impurities, as detected by the XRD method. Therefore, all investigations in the present study were carried out on Bi_2S_3 thin films, as-deposited and thermally treated up to 250 °C during 10 min (i.e. on films not containing impurities in quantities detectable by the XRD methods). As shown in our previous study [15], according to the Debye–Scherrer approach, the as-deposited thin films are nanocrystalline with average crystal radius of 9.0 nm, while upon thermal treatment at 250 °C this value increases to 24.2 nm. The average crystal radii values obtained for bulk precipitates were

identical with the values corresponding to the materials deposited in thin film form, a finding which is in line with the conclusion that the crystal growth predominantly occurs by the cluster mechanism [31].

2.3. Experimental techniques employed in studying the electrical and photoelectrical properties of nanocrystalline bismuth(III) sulfide thin films

To provide ohmic contact with bismuth(III) sulfide thin films, which is essential for studying its electrical and photoelectrical properties, coplanar silver electrodes were applied onto films's surface. The non-rectifying character of the silver–bismuth(III) sulfide contacts was proved on the basis of the measured current–voltage characteristics [32,33].

For measurement of dark electrical resistance of investigated thin films the methods of two- and four-point probes (i.e. the van der Pauw method) [34,35], as well as the constant field method [36] were used.

The dependence of dark electrical resistance of bismuth(III) sulfide thin films on temperature was measured by constant field method, using the setup presented in Fig. 1. These measurements were carried out in inert (argon) atmosphere at $P = 80\,\text{kPa}$.

Spectral dependence of stationary photoconductivity in the case of thermally treated films was measured also employing the constant field method. The type of electrical conductivity was determined using the method based on the thermoelectrical (Seebeck) effect [34,35].

Relaxation dynamics of non-equilibrium (photoexcited) charge carriers, from the kinetic aspect, was investigated using the oscillographic method [16,17,36]. The experimental setup for these measurements is shown in Fig. 2. Much more details about all the electrical measurements performed in the present paper can be found in our previous studies [16,17,19] devoted to these aspects.

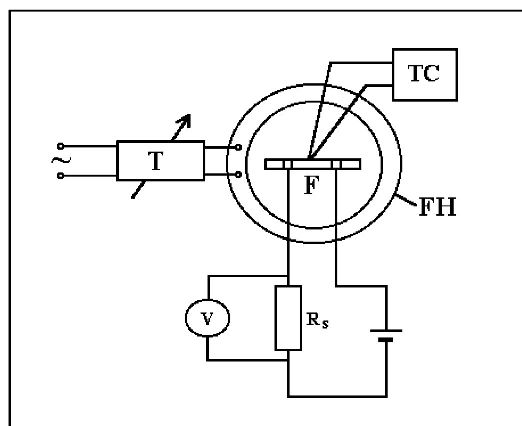

Fig. 1. The experimental setup used for measurements of the temperature dependence of dark electrical resistance of Bi_2S_3 thin films on the basis of the constant field method.

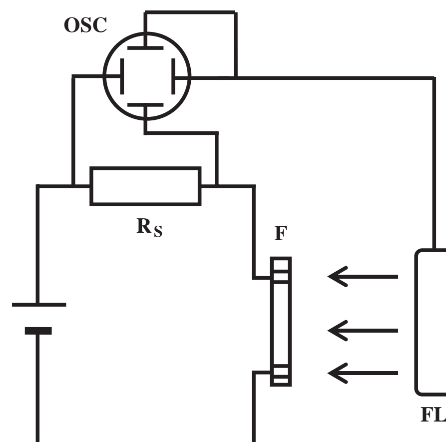

Fig. 2. The experimental setup used for investigation of the relaxation dynamics of non-equilibrium charge carriers in Bi_2S_3 thin films by the oscillographic method.

3. Results and discussion

3.1. Electrical measurements

3.1.1. Ohmic contact with bismuth(III) sulfide thin films

To achieve ohmic contact with bismuth(III) sulfide thin films, silver paste was used. The current–voltage characteristics of silver–bismuth(III) sulfide contact are presented in Fig. 3. As can be seen, I–V dependence is linear within the studied voltage range and this proves that the contact is ohmic. Namely, the derivative $(\partial I/\partial V)^{-1}$ is constant and practically equal to the dark electrical resistance of investigated bismuth(III) sulfide thin film, indicating a negligible value of the contact resistance [32,33]. The non-rectifying character of silver–bismuth(III) sulfide contact is also preserved upon film illumination with white light, which is proven by the measured I–V dependencies at various values of the incident light flux.

3.1.2. Measurements of dark electrical resistance of bismuth(III) sulfide thin films

As mentioned in the previous section, three experimental methods were employed to measure the dark electrical resistances of bismuth(III) sulfide thin film samples: the two-point, four-point probe methods, as well as the constant field method.

When the four-point probe method was applied, the dark electrical resistivity of the investigated samples was calculated on the basis of the following equation [35]:

$$\exp\left(-\pi\frac{d}{\rho}\frac{V_{CD}}{I_{AB}}\right) + \exp\left(-\pi\frac{d}{\rho}\frac{V_{DA}}{I_{BC}}\right) = 1. \tag{1}$$

In (1), d is film's thickness, ρ is the resistivity of semiconducting material, V_{CD} and V_{DA} are the voltage drops between points (C and D) and (D and A)

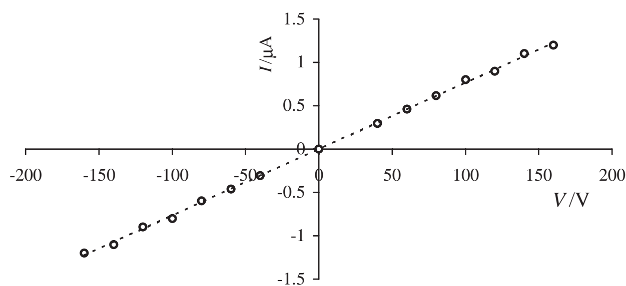

Fig. 3. The current–voltage characteristics of silver–bismuth(III) sulfide contact.

correspondingly, while I_{AB} and I_{BC} are the corresponding electric currents passed between points (A and B) and (B and C), respectively, for the arrangement of contacts within the van der Pauw method [35]. Numerical solutions for ρ were obtained from (1) on the basis of experimental data for other quantities appearing in Eq. (1), employing the generalized reduced gradient (GRG2) non-linear optimization code, as implemented in MS Excel program (i.e. its SOLVER tool for finding numerical solutions of algebraic equations).

The constant field method for measurement of the dark d. c. resistance of the samples was based on mathematical analysis of electrical circuit containing a d.c. source serially connected to the investigated film and a standard resistor. The following equation may be straightforwardly obtained by this analysis [36], relating R to the other parameters of the circuit:

$$R_{\mathrm{f}} = \frac{V_{\mathrm{b}} R_{\mathrm{s}}}{V_{\mathrm{s}}} - R_{\mathrm{s}}, \tag{2}$$

where V_b is the applied voltage and V_s is the voltage drop at the ends of the standard resistor with the resistance R_s, while R_f is the investigated film resistance. In cases when $R_s \ll R_f$, the dark electrical resistance of thin film sample is related to the other experimental observables by a much simplified form of Eq. (2):

$$R_{\mathrm{f}} = \frac{V_{\mathrm{b}} R_{\mathrm{s}}}{V_{\mathrm{s}}}. \tag{3}$$

The last equation is in fact the basis of the constant field method. We provided the condition $R_s \ll R_f$ in all of the measurements carried out for the purpose of this study, by controlling the R_s value. The measured dark electrical resistances of thin film samples using the two-point, four-point probe methods, as well as the constant field method are in excellent agreement.

In general, it has been well recognized that the electrical resistivity of a polycrystalline thin film material is strongly dependent on the conditions under which that material has been prepared. The previous statement is especially important when one deals with nanocrystalline materials (as in the present case). This is so since in the case of nanocrystalline materials, due to the relatively high surface area, the contacts between nanoparticles play a crucial role in determination of their electrical properties. For an ensemble of quantum dots deposited in thin film form, due to the relatively high surface area, it would be expected that the electrical transport is barrier-dominated. The existence of potential barriers at the crystalline (i.e. grain) boundaries may be attributed to the band bending at the nanocrystal surfaces (Fig. 4). For such a case, the conductivity is given by [37]:

$$\sigma = \frac{Ne^2\langle v\rangle}{4kT} \cdot L \cdot \exp\left(-\frac{e\phi}{kT}\right). \tag{4}$$

In the previous equation, N denotes the carrier number concentration within the nanocrystals (electrons in the present case), $\langle v\rangle$ is the average thermal velocity of free carriers, L is the average distance between barriers, ϕ is the barrier potential, while e, k and T are the electron charge, Boltzmann constant and thermodynamic temperature, respectively.

The as-deposited Bi_2S_3 thin films are nanocrystalline with average crystal radius of 9.0 nm [15]. Upon thermal treatment at 250 °C, this value increases to 24.2 nm [15]. Such increase of the average nanocrystal size upon thermal annealing treatment is due to coalescence and crystal growth. It is followed by irreversible loss of confinement effects. Electrical resistance of as-deposited films is of the order of magnitude of about 10 GΩ (from 20 to 50), depending on the film thickness and the exact conditions of chemical deposition process. The resistance is inversely proportional to the film thickness, although after some limiting thickness it tends to a constant value. We further discuss in somewhat more details the dependence of electrical resistance of the films on the composition of the deposition solution and the post-deposition annealing treatment. The unannealed (as-deposited) Bi_2S_3 films are not photoconductive. Upon thermal treatment, the resistivity decreases by 3–4 orders of magnitude, and the thermally treated films manifest pronounced photoconductive properties. In the framework of the grain boundary effects concept, taking into consideration Eq. (4), it is quite clear which are the main reasons behind the increase of σ (i.e. decrease of ρ and R) upon thermal treatment. On one hand, due to the average crystal size increase, the average distance between barriers L in Eq. (4) increases, which clearly leads to increase in σ. On the other hand, thermal treatment may also lead to decrease in the barrier height $e\phi$ [37]. In the present study, employing Eq. (4), we tried to estimate the exact magnitude of barrier height decrease upon thermal treatment of the films, leading to average crystal size increase. If the free carrier concentrations and their average thermal velocities are presumed to remain constant upon annealing, the ratio

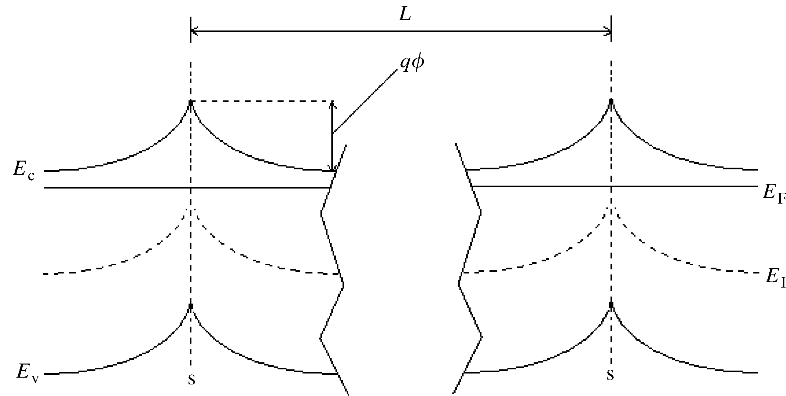

Fig. 4. A schematic presentation of the existence of potential barriers at the intercrystalline (i.e. grain) boundaries due to band bending on the nanocrystal surfaces.

between film conductivities before and after annealing is given by:

$$\frac{\sigma_{\text{as-dep.}}}{\sigma_{\text{annealed}}} = \frac{L_{\text{as-dep.}}}{L_{\text{annealed}}} \cdot \exp\left[\frac{(e\phi)_{\text{annealed}} - (e\phi)_{\text{as-dep.}}}{kT}\right]. \quad (5)$$

Since the ratio $L_{\text{as-dep.}}/L_{\text{annealed}}$ may be regarded as practically equal to the ratio of average crystal sizes before and after annealing (determined from the XRD studies), on the basis of the measured changes in conductivities the barrier height decrease upon thermal treatment may be estimated from (5). On the basis of our experimental data, the estimated $(e\phi)_{\text{annealed}} - (e\phi)_{\text{as-dep.}}$ value is 3.38×10^{-20} J (0.21 eV).

Regarding the dependence of the measured electrical resistivity on the composition of the deposition solution and the experimental conditions of the deposition process, it may be attributed primarily to the influences of these variables on the purity of obtained bismuth(III) sulfide. Inclusion of any other phases (such as bismuth(III) oxide) in an even very small quantities within the Bi_2S_3 films (which may be under detection limit of XRD analysis) act as impurities with chemical character. Their presence in band structure is manifested through discrete impurity levels in the forbidden band [38], which are almost completely ionized at room temperature ($\approx$300 K). As a result of ionization of impurity levels, the equilibrium concentrations of charge carriers increases and dark electrical resistance decreases. Any significant increase of the pH value of the deposition solution from the optimal one [15] would, e.g., increase the possibility of inclusion of oxide phases within the deposited films. On the other hand, any significant decrease of pH would in principle increase the possibility of more significant generation of elemental sulfur in the reaction system (see Ref. [15] for a detailed analysis of all the existing chemical equilibria in the reaction system), which could also incorporate as chemical impurity within the films. It is, however, worth noting that in order to achieve optimal photoelectrical performances of the deposited nanocrystalline films, it is of essential importance to carefully control all the previously mentioned factors influencing these properties. Thus, on one hand, the annealed Bi_2S_3 thin films exhibiting maximum photoconduction response may be regarded as being very close to ideal stoichiometrical composition, and thus characterized by relatively high resistivity (i.e. act as intrinsic semiconductors). Any more significant deviation from the ideal crystal structure (such as an increased number of point or line defects, or even vacancies or interstitial atoms), as well as incorporation of any other impurities of physical or chemical character in significant quantities, may lead to appreciable reduction of electrical resistivity of the samples, which degrades significantly their photoelectrical properties. On the other hand, in the case of very small (as-deposited) nanocrystals, for which the electrical resistivities are rather high (as elaborated before in this chapter) due to the large grain boundary barriers and small L values, again the photoelectrical response is essentially negligible. It is therefore a rather difficult task to precisely control the experimental deposition conditions as well as the post-deposition treatment in order to obtain samples with optimal photoconductive performances.

3.1.3. *Determination of type of electrical conductivity of Bi_2S_3 nanocrystalline thin films*

On the basis of the thermoelectric force measurements (the hot point probe method), i.e., from the obtained sign of the thermoelectric force of Bi_2S_3-metal thermocouple, it was concluded that the dominant charge carriers in this semiconductor are electrons. This is in line with the results from previous studies of this semiconducting material [1–12]. It has been often stated as a generalized experience from a number of experimental studies that it has been shown to be impossible to prepare this material in form of a p-doped semiconductor.

3.1.4. Determination of thermal band gap energy and ionization energies of impurity levels of photoconductive Bi_2S_3 nanocrystals deposited in thin film form

To determine the thermal band gap energy and the ionization energies of the impurity levels in the case of studied bismuth(III) sulfide semiconducting nanocrystals in thin film form, we have measured the temperature dependence of their dark electrical resistivity.

As may be shown from the solid-state theory of semiconductors [34,35,38], in case of a semiconductor with only one impurity level, the temperature dependence of dark electrical resistance is given by

$$R(T) = R_0 \cdot \exp\left(\frac{E_g}{2kT}\right) + R_0' \cdot \exp\left(\frac{\Delta E}{kT}\right). \tag{6}$$

In previous equation, R_0 and R_0' are constants, E_g is the thermal band gap energy, ΔE is the impurity level ionization energy, k is Boltzmann constant, and T is temperature. The overall temperature dependence of the electrical resistivity of semiconducting samples is therefore expressed through the exponential terms, although rigorously speaking, the parameter R_0 in fact contains a term which is temperature dependent, but very weakly [38]. If a semiconducting material exhibits a temperature dependence of R governed by Eq. (6), it is often stated that the direct current conductivity exhibits an Arrhenius-type behavior, with activated-type conduction. Generalization of Eq. (6) in case of a semiconductor having more than one impurity levels is straightforward:

$$R(T) = R_0 \cdot \exp\left(\frac{E_g}{2kT}\right) + \sum_{i=1}^{n} R_{0,i}' \cdot \exp\left(\frac{\Delta E_i}{kT}\right). \tag{7}$$

In the region of relatively lower temperatures, the overall conductivity of the semiconductor samples is dominated by the charge carriers generated by ionization of impurity levels (extrinsic conductivity), and thus the second term in Eq. (6) prevails in the $R(T)$ dependence. At sufficiently higher temperatures, on the other hand, the temperature dependence of conductivity is dominated by the band-to-band electronic transitions. Under such conditions, the charge carriers acquire enough thermal energy to make an interband transition (the intrinsic conductivity is "activated" at these temperatures). In the sense of previous discussion, the two terms appearing in Eq. (6) may be treated independently in the corresponding temperature intervals. We have therefore carried out the analysis of our experimental data according to the previously outlined arguments.

In line with the previous discussion, if one considers the dependence of $\ln(R)$ on $1/T$, the number of linear trends appearing in it is a clear indication of the number of impurity levels within the forbidden band (the so-called band gap states).

The dependence of $\ln(R)$ on $1/T$ in the temperature interval from 10 °C to 300 °C for a Bi_2S_3 thin film sample is shown in Fig. 5. As obvious from this figure, two linear trends are clearly observable in this dependence, indicating the existence of only one impurity band gap level in the case of the studied semiconducting material. In the higher temperature interval (from about 170 °C to 300 °C), the overall $R(T)$ dependence is predominated by the intrinsic charge carriers generation, and is therefore to a good approximation given by

$$R(T) = R_0 \cdot \exp\left(\frac{E_g}{2kT}\right). \tag{8}$$

Taking the natural logarithm of both sides of Eq. (8) and differentiating with respect to $1/T$, one arrives at the following expression for the thermal band gap energy:

$$E_g = 2k\frac{\mathrm{d}\ln(R(T))}{\mathrm{d}(1/\mathrm{T})}. \tag{9}$$

This parameter was therefore calculated from the slope of $\ln(R)$ vs. $1/T$ dependence, obtained from a linear

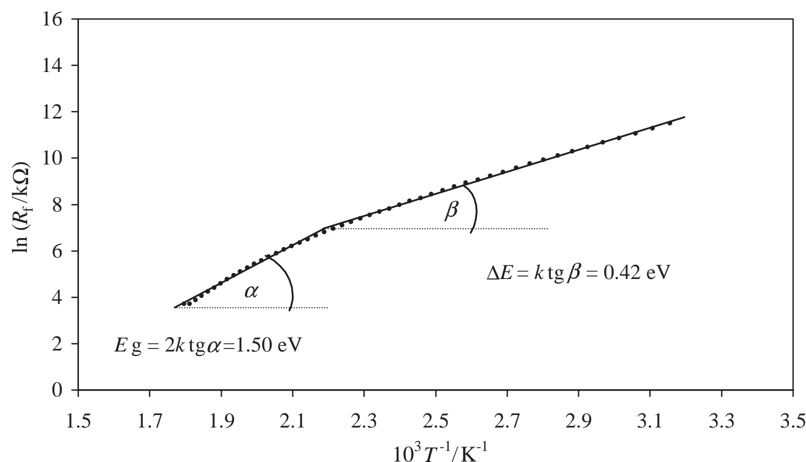

Fig. 5. The dependence of $\ln R$ on $1/T$ in the temperature interval from 10 °C to 300 °C for a Bi_2S_3 thin film sample.

regression analysis of our experimental data within the temperature interval of intrinsic conductivity. The obtained value for E_g is 1.50 eV. This value is in very good agreement with the one obtained from optical spectroscopy measurements (1.61 eV [15]). However, exact matching of these two values is not expected, since the optical band gap value refers to room temperature, while the thermal one (as can be shown from the solid state theory [34,35,38]) refers to 0 K. These findings imply the possibility that the derivative $\partial E_g/\partial T$ is positive for the studied material, a case which seems to be different from most of the common semiconducting materials (although certain cases characterized with $\partial E_g/\partial T > 0$ are known in the literature). However, since the physical meaning of the thermal band gap value is in a sense obtained by an extrapolation procedure, in order to confirm such an implication, exact variable-temperature measurements of optical spectra of Bi_2S_3 thin films are required. We will devote a separate study to this subject.

The decrease of thin film dark resistance upon increase of temperature in the region of extrinsic conductivity (corresponding to the lower temperature interval) follows the equation:

$$R(T) = R'_0 \cdot \exp\left(\frac{\Delta E}{kT}\right). \tag{10}$$

Similarly as in the case of E_g, taking the natural logarithm of Eq. (10) and subsequently differentiating with respect to $1/T$, the following expression is obtained for the impurity level ionization energy:

$$\Delta E = k\frac{\mathrm{d}\ln(R(T))}{\mathrm{d}(1/T)}. \tag{11}$$

On the basis of the slope of $\ln(R)$ vs. $1/T$ dependence in the temperature region of extrinsic conductivity mechanism, obtained from a linear regression analysis of the experimental data the value of 0.42 eV is obtained for the impurity-level ionization energy. This level is in fact a donor level, having in mind the previously discussed type of conductivity of the studied material.

The reproducibility of the measurements of temperature dependence of dark electrical resistance was proven by comparison of data obtained during multiple heating–cooling cycles. In Fig. 6 the dependence of $\ln R$ vs. $1/T$ during a single heating–cooling cycle is presented. The slight differences between the exact resistance values measured at a given temperature during heating and cooling may be attributed to the fact that the heating process is usually performed quite faster (due to purely instrumental reasons) than the cooling, which is usually left to occur spontaneously. However, these very slight differences do not substantially affect the calculated thermal band gap energy and impurity-level ionization energy. The presented values were, however, calculated from the data obtained from measurements during the cooling process, since as already mentioned it is carried out more slowly and the voltage drop measurements at any particular temperature value are considered to be more reliable.

3.2. Photoelectrical measurements

3.2.1. Spectral dependence of photoconductivity of nanocrystalline bismuth(III) sulfide thin films

The study of the phenomenon of photoconductivity is an effective method for understanding band structures of investigated semiconducting materials [6,28,37,39–57]. Using the photoconductivity measurements, information about kinetics of generation, transport and recombination of charge carriers, as well as the density and nature of states in the energy gap due to the presence of impurities and defects can be obtained [39–57]. The phenomenon of photoconductivity of semiconductors is due to the intrinsic photoeffect i.e. to the interaction with electromagnetic radiation from

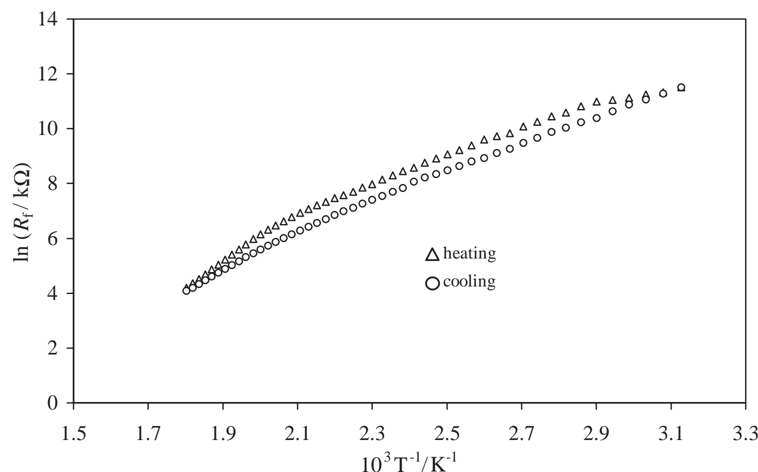

Fig. 6. The dependence of $\ln R$ vs. $1/T$ during a single heating–cooling cycle for a Bi_2S_3 thin film sample.

the intrinsic region of investigated semiconducting material which is followed by generation and recombination of non-equilibrium (photoexcited) charge carriers. Under stationary conditions the rates of these two processes are equal and the photoconductivity (or non-equilibrium conductivity) is constant [34,36].

To measure the spectral dependence of stationary photoconductivity, we have constructed a setup containing a d.c. source serially connected to a standard resistor and the investigated thin film sample of bismuth(III) sulfide. As a source of radiation we have used a monochromator from spectrophotometer Beckman DU-2 within the wavelength range from 400 to 1200 nm. The samples used for photoconductivity measurements were previously appropriately prepared. They were characterized with length of 4 mm and width of 3 mm. For ohmic contact with investigated material two coplanar silver electrodes were put 4 mm apart [17].

As can be shown by mathematical analysis of the employed electric circuit in these experimental measurements, the stationary photoconductivity depends on dark electrical resistance of the investigated sample (r_0) and resistance of the standard resistor (R) according to the following equation:

$$\Delta\sigma_{\mathrm{st.}} = \frac{v \cdot (R + r_0)^2}{r_0^2 VR - vr_0 R \cdot (r_0 + R)}, \tag{12}$$

where V is the applied voltage and v is the voltage drop at the end of the standard resistor. In the case of constant field method ($R \ll r_0$), Eq. (12) may be simply rearranged to the following form:

$$\Delta\sigma_{\mathrm{st.}} = \frac{v}{R \cdot V}. \tag{13}$$

As implied by the last equation, the stationary photoconductivity is proportional to the voltage drop v. Therefore, the experimental measurements of spectral dependence of stationary photoconductivity were based on registration of the voltage drop (v) at the ends of the standard resistor during interaction between the investigated sample and monochromatic radiation.

According to our experiments, as-deposited bismuth(III) sulfide thin films are non-photoconductive. After thermal treatment at 250 °C in air atmosphere for about 10 min they manifest the phenomenon of photoconductivity. As we have discussed in our previous paper [15], the as-deposited bismuth(III) sulfide thin films are nanocrystalline with average crystal radius of 9.0 nm estimated within the framework of Debye–Scherrer approach. The absence of photoconductivity of unannealed thin films is due to strongly manifested grain boundary effect i.e. to the localization of electrons and holes in a three-dimensionally confined space (quantum dot). Upon thermal treatment at 250 °C, as a result of coalescence and crystal growth processes, the average crystal radius of bismuth(III) sulfide increases to 24.2 nm. This is accompanied by electrical connection of nanocrystals and weakening of grain boundary effects.

In Fig. 7, the spectral dependence of stationary photoconductivity of bismuth(III) sulfide thin film is presented. As can be seen, the investigated sample manifests maximal photoconductivity upon interaction with monochromatic radiation with wavelength of 770 nm. The red absorption edge of registered photoconductivity occurs at about 1.10 eV. Upon interaction with photons with energies higher than band gap energy of investigated material, as a result of intensive surface absorption the concentration of non-equilibrium charge carriers (photocarriers) increases. On the other hand, the high concentration of photocarriers favors the annihilation processes and decrease of photocarrier's lifetime and therefore the photoconductivity as well. This effect is known in the literature as *surface relaxation process* [32].

3.2.2. Determination of optical band gap energy of photoconductive Bi_2S_3 thin films on the basis of photoconductivity spectrum

Using the recorded spectral dependence of stationary photoconductivity, on the basis of photon energy which corresponds to maximal photoconductivity, we have obtained a band gap energy of 1.61 eV for synthesized

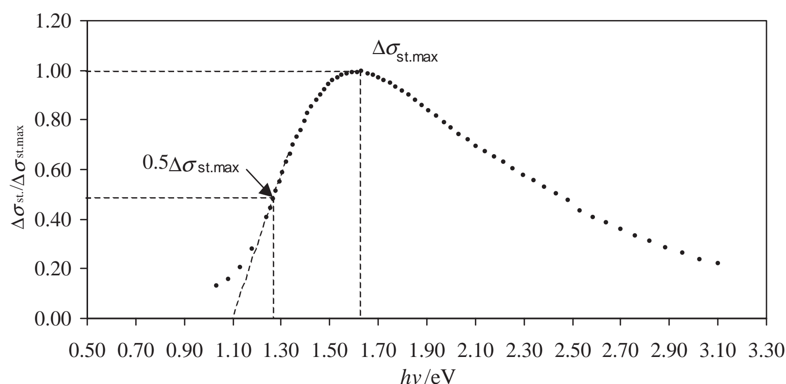

Fig. 7. The spectral dependence of stationary photoconductivity for a bismuth(III) sulfide thin film sample.

thin film material (see Fig. 7). This value is in excellent agreement with that calculated on the basis of absorption spectrum using the Fermi's golden rule for fundamental interband electronic transitions in case of a parabolic energy structure [15].

In the limit of relatively low absorption, it can be shown that the photoconductivity spectrum (represented by the dependence of $\Delta\sigma$ or $\Delta\sigma/\Delta\sigma_{\max}$. on $h\nu$) is in fact proportional to the absorption spectrum. In fact, the photoconductivity, i.e., the $\Delta\sigma$ value is proportional to the number of photons absorbed by the investigated thin film. The last value is, on the other hand, proportional to the decrease of the intensity of incident light upon absorption by the film of thickness d:

$$\int_0^d |\mathrm{d}I| \cdot \mathrm{d}x. \tag{14}$$

However, since:

$$|\mathrm{d}I| = \alpha I_0 \cdot \exp(-\alpha x)\,\mathrm{d}x \tag{15}$$

one straightforwardly arrives at

$$\Delta\sigma \propto \alpha I_0 \cdot \int_0^d \exp(-\alpha x)\,\mathrm{d}x = (1 - \exp(\alpha \cdot d)). \tag{16}$$

The last expression reduces to $\alpha\ d$ in the limit of low values of the term in the exponential function (the limit of low absorption), i.e. $(1 - \exp(\alpha \cdot d)) \approx \alpha \cdot d$. Finally, one arrives at the conclusion that in the low absorption limit the relation $\Delta\sigma \propto \alpha \cdot d$ holds.

The last conclusion has a number of important consequences. It allows the band gap energy of a semiconducting material to be calculated employing the expressions arising from the Fermi's golden rule for band-to-band transitions on the basis of parabolic approximation for the dispersion relation. This may be done by simply replacing the function $\alpha(h \cdot \nu)$ by $\Delta\sigma(h\nu)$, as the two functions are directly proportional in the limit of low absorption. We have therefore constructed the dependencies of $(\Delta\sigma \cdot h \cdot \nu)^n$ on $h \cdot \nu$ for various values of the exponent n. A clearly manifested linear dependence in a wide energy region was obtained in case of $n = 2$. This finding indicates that the band-to-band electronic transitions in the case of studied Bi_2S_3 thin films are of a direct type, i.e., they do not involve a change in electronic momentum upon transition. In other words, the absolute minimum of the valence band and the absolute maximum of the conduction band correspond to the same point in the k-space, and no phonons are required for the electron momentum to be preserved in the course of transition. These results are in agreement with the conclusions derived in our previous paper on the basis of UV-VIS spectra of the studied material. Similarly, as in the analysis of the optical spectroscopy data presented in our previous papers [15–25], we have carefully carried out linear least-squares fits of the $(\Delta\sigma \cdot h \cdot \nu)^2$ vs. $h \cdot \nu$ dependencies in the relevant energy ranges (with successive inclusion or elimination of a number of neighboring points in the correlation ranges) and parallel we have monitored the R^2 value. Thus, the sets of relevant points belonging to the linear $(\Delta\sigma \cdot h \cdot \nu)^2$ vs. $h \cdot \nu$ dependency originating from a given band-to-band transition were determined. Finally, we have extrapolated $(\Delta\sigma \cdot h \cdot \nu)^2$ vs. $h \cdot \nu$ dependences to $\Delta\sigma \cdot h \cdot \nu = 0$ and we have determined the corresponding transition energies, on the basis of previously derived correlation equation of the form:

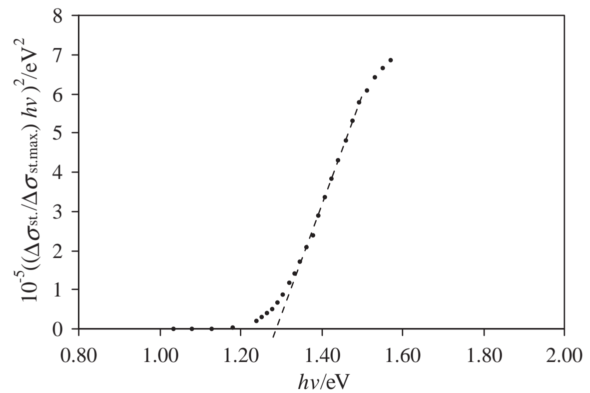

Fig. 8. Determination of the band gap energy of a Bi_2S_3 thin film sample on the basis of its photoconductivity spectrum using the parabolic approximation for the dispersion relation. The analysis of photoconductivity spectrum is carried out employing the principle of correspondence between th photoconductivity and absorption spectra in the limit of low absorption.

$$(\Delta\sigma \cdot h \cdot \nu)^2 = \mathrm{const} \cdot (h \cdot \nu - E_g). \tag{17}$$

According to this procedure, the value of 1.30 eV is obtained for the band gap energy of the investigated material (Fig. 8). This value is also in very good agreement with the one obtained from analysis of the optical absorption spectroscopy data for this system reported in our previous study (1.61 eV [15]). Another method which has been often employed in the literature to determine the optical band gap energy of semiconducting materials from their photoconductivity spectra is the one based on determination of the energy at which the photoconductivity response acquires half of its maximum value. In the case of presently studied material, the band gap energy obtained by this procedure ($\approx$1.30 eV, see Fig. 7) is in excellent agreement with the one determined on the basis of Eq. (17), i.e., on the equivalence of absorption and photoconductivity spectra in the low absorption limit.

3.2.3. *Relaxation dynamics of photoexcited non-equilibrium charge carriers in Bi_2S_3 nanocrystals deposited in thin film form*

Another aspect, which is of particular importance for the potential application of the studied material in the field of opto- and microelectronics is the time decay of

non-equilibrium conductivity (photoconductivity). The time constant determining the overall kinetics of the photoconductivity decay process is a rather relevant parameter which basically determines the most appropriate usage of the studied material. In the present study, we have investigated the relaxation dynamics of non-equilibrium charge carriers (i.e. photo-carriers) using the oscilloscopic method. The experimental setup [17] employed for the oscilloscopic pump-probe experiments is schematically depicted in Fig. 2. The photoexcitation of the investigated material in thin film form was achieved by illumination with a flash lamp characterized with the decay of the lamp pulse of about 20 μs. Investigated film was serially connected to a standard resistor R_s. The time dependence of the voltage drop at the ends of the standard resistor was followed by transferring this signal to an oscilloscope with previously calibrated time and voltage axes. From the digitalized $\Delta v = f(t)$ function, the electrical resistance (and therefore also the non-equilibrium conductivity $\Delta\sigma(t)$) of investigated thin film at each sampled value of t was calculated according to the constant field method.

The phenomena of recombination (or relaxation) of non-equilibrium charge carriers in semiconducting materials may be classified from various viewpoints [36]. From the viewpoint of the nature of energy released during this processes, the recombination phenomena are usually classified as radiative or non-radiative. In the first case, the energy is released through emission of photons, while in the second case it is dissipated to the lattice in the form of heat. On the other hand, from a purely kinetic viewpoint, the non-equilibrium charge carriers may be relaxed (recombined) according to the linear or quadratic mechanism. It is the second aspect that we investigate more thoroughly in the present study.

A recorded oscillogram for a Bi_2S_3 thin film annealed at 250 °C for 10 min is shown in Fig. 9. Employing the constant field method (Eq. (13) in Section 3.2.1), on the basis of the measured time dependence of the voltage drop at the ends of the standard resistor R_s, the corresponding relaxation curve (the time-dependent non-equilibrium conductivity, i.e., photoconductivity function) was constructed. The experimental data from dependence $\Delta\sigma/\Delta\sigma_{max} = f(t)$ were further analyzed by interpolation with functions determining the time dependence of photocarrier's concentration in the case of linear and quadratic recombination processes regimes.

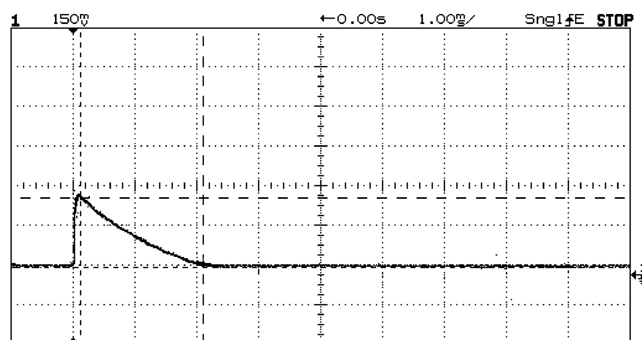

Fig. 9. A recorded oscillogram for a Bi_2S_3 thin film annealed at 250 °C for 10 min after the interaction with electromagnetic radiation is switched off.

If one considers photoexcitation with Heaviside-type rectangular light impulses (the Heaviside approximation for the pumping light impulse is quite valid in cases when time constant of the lamp signal decay is significantly smaller than the time constant of the non-equilibrium charge carrier decay), the overall dynamics of non-equilibrium charge carriers is governed by the following differential equation [36,57]:

$$\frac{d(\Delta N)}{dt} = v_{gen.} - v_{rec.}. \tag{18}$$

In Eq. (18), ΔN denotes the excess number concentration of charge carriers with respect to the equilibrium value (i.e. the concentration of photogenerated charge carriers), $v_{gen.}$ denotes the rate of charge-carriers generation, while $v_{rec.}$ is the rate of their recombination. In the case of linear recombination mechanism, only one type of charge carriers are relevant for the overall recombination kinetics, the rate of recombination being proportional to their actual concentration. The proportionality constant in this case is the reciprocal of the average lifetime of photogenerated charge carriers—τ. The solution of the ordinary linear differential equation (18) for a general case in which both generation and recombination processes occur has the form:

$$\Delta N(t) = \Delta N_{st.}(1 - e^{-t/\tau}), \tag{19}$$

where $\Delta N_{st.}$ is the stationary value of the photogenerated charge carriers concentration ($\Delta N_{st.} = \tau \cdot \beta \cdot \alpha \cdot I$, where I is the intensity of the incident light, α is the absorption coefficient of the investigated material, while β is the quantum yield).

When the light impulse is switched off ($v_{gen.} = 0$), the solution of (18) takes the form:

$$\Delta N(t) = \Delta N_{st.} \cdot e^{-t/\tau}. \tag{20}$$

Since $\Delta\sigma$ is proportional to ΔN, for the first-order relaxation kinetics the $\Delta\sigma(t)$ dependence is given by

$$\Delta\sigma(t) = \Delta\sigma_{st.} \cdot e^{-t/\tau}. \tag{21}$$

If the relaxation process is kinetically of a second order ($v_{rec.} = \gamma \cdot \Delta N_c \cdot \Delta N_h$, where ΔN_e and ΔN_h denote the number concentrations of photogenerated electrons and holes, respectively, while γ is the recombination coefficient), then upon light impulse switch off the solution of

(18) has the form:

$$\Delta N(t) = \sqrt{\frac{\alpha \cdot \beta \cdot I}{\gamma}} \frac{1}{t\sqrt{\alpha \cdot \beta \cdot \gamma \cdot I} + 1}. \quad (22)$$

Similar expressions govern the rise or decay of $\Delta\sigma$, i.e., the function $\Delta\sigma(t)$.

From the dependence $\Delta\sigma/\Delta\sigma_{\max} = f(t)$ obtained on the basis of experimental oscillographic data, we have constructed the dependencies of $\ln(\Delta\sigma)$ and $1/\Delta\sigma$ on t. A linear dependence was obtained only in the first case (Fig. 10), indicating that the non-equilibrium charge carrier recombination occurs through the linear relaxation mechanism. The average lifetime (i.e. relaxation time) of non-equilibrium charge carriers in photoexcited Bi_2S_3 nanocrystals deposited in thin film form, calculated on the basis of slope of $\ln(\Delta\sigma)$ as a function of t (i.e. the value of the derivative $\mathrm{d}\ln(\Delta\sigma)/\mathrm{d}t; \mathrm{d}\ln(\Delta\sigma)/\mathrm{d}t = -1/\tau$) is 1.58 ms. This value is in very good agreement with the recently reported value of 1.65 ms for Bi_2S_3 thin films obtained by spray pyrolysis technique [2]. Our conclusions about the type of relaxation mechanism are in line with the data presented in this study, too. The calculated relatively high value of the photocarrier's lifetime (on an absolute scale) implies that the obtained Bi_2S_3 nanocrystals in thin film form have a potential application in fabrication of solar cells.

According to the values of the band gap energy of the studied material in thin film form, as well as of the photocarrier's lifetime and type of relaxation mechanism, it may be concluded that relaxation (i.e. recombination) processes occur via local trapping centers. As we have detected the existence of a single donor level in the forbidden band from the measured temperature dependence of dark resistivity of studied Bi_2S_3 films, it is probably exactly this level that determines the charge carrier recombination kinetics. Recombination processes occurring via a single-type trapping center can be described within the framework of the Schockley–Read model [36].

If one considers multiple-type trapping centers as being responsible for the photoconductivity relaxation, kinetic analysis of these phenomena leads to the following expression for the effective relaxation time of non-equilibrium charge carriers (τ):

$$\frac{1}{\tau} = \sum_k \frac{1}{\tau_k}. \quad (23)$$

In the previous equation, τ_k is the non-equilibrium charge carrier lifetime with respect to the kth capturing level. Each τ_k is defined with:

$$\tau_k = \frac{1}{q_k v_k p_k}, \quad (24)$$

where v_k is the charge carrier's velocity, q_k the capture cross-section and p_k is the number concentration of the corresponding trapping center. Expression (24) in principle allows the capture cross-section to be calculated from photoconductivity relaxation measurements (i.e. from the obtained τ values) if the data for v_k and p_k are available. In the present case, however, reliable data for p_k and v_k have not yet been provided, thus somehow obscuring the possibility to calculate a reliable value for the capture cross-section. However, we note once again in this context that the photocarrier's relaxation time value determined from photoconductivity relaxation data in the present study is in very good agreement with the recently reported value of 1.65 ms for Bi_2S_3 thin films obtained by spray pyrolysis technique [2]. Although the capture cross-section values have not been reported in [2] as well, taking into account the other parameters of the polycrystalline films investigated in this paper, the corresponding capture cross-section values are expected to be rather close.

As can be seen from the oscillogram presented in Fig. 9, the obtained Bi_2S_3 thin films do not manifest residual photoconductivity.

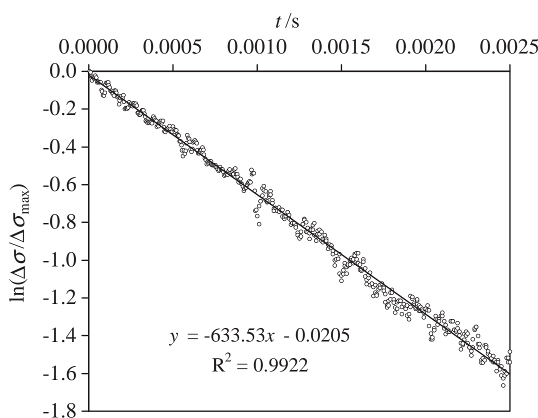

Fig. 10. The dependence of $\ln(\Delta\sigma)$ on t obtained on the basis of experimental oscillographic data for a Bi_2S_3 thin film.

3.2.4. *Dependence of non-equilibrium conductivity on the intensity of incident light (the lux–ampere characteristics) in the case of photoconductive Bi_2S_3 thin films*

In order to provide further experimental data about the recombination mechanism of non-equilibrium charge carriers in the case of studied Bi_2S_3 thin films, we have measured the dependence of non-equilibrium conductivity on the intensity of incident light (i.e. the lux–ampere characteristics of the material). We have used a source of white non-polarized light for these measurements. The excess conductivity (photoconductivity) was measured using the constant field method, modulating the incident light intensity (and its flux and illumination of the sample correspondingly) by changing the distance between light source and the investigated

thin film. The incident light flux (or, more precisely, the illumination of the sample) was measured by a MASTECH MS 6610 luxmeter.

The photoconductive properties of a given material in both static and dynamical (i.e. kinetic) sense are governed by carrier localization/delocalization processes. Gaining further knowledge about the localized states in semiconducting materials may thus throw additional light on the mechanism of photosensitivity of the materials in question. This, on the other hand, is of certain importance for application of the studied material in fabrication of various photosensitive devices.

In a general case, it can be shown that photoconductivity ($\Delta\sigma$) can be expressed as a power function of the light intensity (I) or the flux of the incident light (Φ) [36,41,42,58]:

$$\Delta\sigma \sim I^k, \tag{25}$$

$$\Delta\sigma \sim \Phi^k. \tag{26}$$

In previous equations, k is 1 or 1/2, depending on the type of relaxation mechanism (linear or quadratic, correspondingly). However, it has been often found that k lies in the interval between 0.5 and 1. The case of $0.5<k<1$ is often referred to as a sublinear behavior. According to the several models proposed in the literature for such a regime [41,42,58], a value of the exponent k between 0.5 and 1 strongly indicates an exponential distribution of impurity levels in the forbidden band (the so-called exponential trap distribution). In other words, the trap states density exhibits an exponential dependence on energy [41,42,58]. The value of exponent k is temperature dependent and is given by

$$k = \frac{T^*}{T^* + T}, \tag{27}$$

where T^* is a parameter describing the exponential trap distribution. As obvious from Eq. (27), when $T^* \gg T$, k tends to 1.

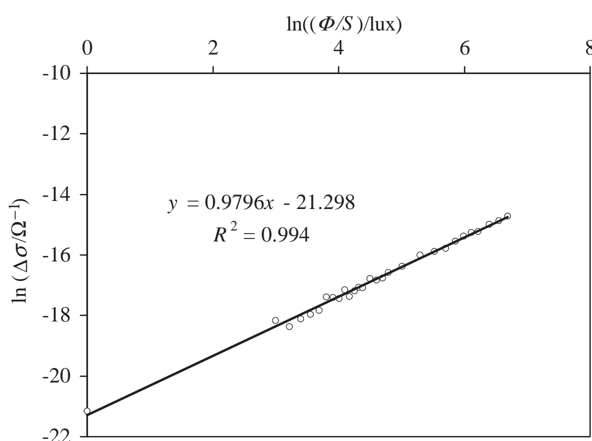

Fig. 11. The dependence of $\ln(\Delta\sigma)$ on $\ln(\Phi/S)$ for a Bi_2S_3 thin film.

On the basis of dependence of $\ln(\Delta\sigma)$ on $\ln \Phi$ (or more precisely $\ln(\Phi/S)$, where S is the illuminated surface area of the film, presented in Fig. 11) the calculated value of k on the basis of linear least-squares fit of experimental data is 0.98. According to these findings, in cumulative relaxation processes the linear mechanism has a dominant role.

4. Conclusions

The charge carriers' transport properties of nanocrystalline semiconducting bismuth(III) sulfide thin films synthesized by chemical deposition method were investigated. These investigations included a study of electrical and photoelectrical properties of the films. Photoconductive performances of nanocrystalline bismuth(III) sulfide films were optimized by physical and chemical means. Post-deposition thermal annealing treatment of as-deposited Bi_2S_3 quantum dots in thin film form leads to electrical connection between nanoparticles and irreversibile loss of confinement effects. To measure the dark electrical resistance of the investigated films, the two-point, four-point probe methods, as well as the constant field method were employed. Silver paste was used to achieve ohmic contact with the films, proving the non-rectifying character of the metal–semiconductor contacts on the basis of the measured current–voltage characteristics. The Seebeck-effect-based hot probe method was used to determine the type of major charge carriers in the obtained films. On the basis of the experimentally measured temperature dependence of the electrical resistance of the films, thermal band gap energy and activation energy of impurity levels were calculated.

The photoconductivity spectra of the films were measured using the constant field method. On the basis of the spectral dependence of the photoconductivity response, the band gap energies of the films were calculated, employing several approaches. The dynamics of recombination of the non-equilibrium charge carriers in photoexcited Bi_2S_3 nanocrystals deposited in thin film form was studied using the oscillographic method. On the basis of the obtained relaxation curves conclusions about the mechanism of relaxation (from the kinetic aspect) were derived and the phenomenological parameter τ (relaxation time) was calculated. The calculated relatively high value of the photocarrier's lifetime (1.58 ms) is in very good agreement with the available experimental data for this material and implies that the obtained Bi_2S_3 nanocrystals in thin film form have a potential application in fabrication of solar cells. According to the band gap energy value of the studied material and the value of the corresponding photocarrier's lifetime and type of relaxation mechanism, it may be concluded that relaxation processes occur via

local trapping centers. Recombination processes occurring via a single-type trapping center can be described within the framework of the Schockley–Read model. According to the measured lux–ampere characteristics of the studied films, in cumulative charge carriers' relaxation processes the linear mechanism has a dominant role.

References

[1] D.J. Riley, J.P. Waggett, K.G.U. Wijayantha, J. Mater. Chem. 14 (2004) 704.
[2] Z. Kebbab, N. Benramdane, M. Medles, A. Bouzidi, H. Tabet-Derraz, Sol. Energy Mater. Sol. Cells 71 (2002) 449.
[3] S.R. Gadakh, C.H. Bhosale, Mater. Res. Bull. 35 (2000) 1097.
[4] R.S. Mane, B.R. Sankapal, C.D. Lokhande, Mater. Res. Bull. 35 (2000) 587.
[5] M.E. Rincon, J. Campos, R. Suarez, J. Phys. Chem. Solids 60 (1999) 385.
[6] R.S. Mane, B.R. Sankapal, C.D. Lokhande, Mater. Chem. Phys. 60 (1999) 158.
[7] N. Benramdane, M. Latreche, H. Tabet, M. Boukhalfa, Z. Kebbab, A. Bouzidi, Mater. Sci. Eng. B 64 (1999) 84.
[8] M. Iovu, S. Shutov, S. Rebeja, E. Kolomeyko, Phys. Status Solidi (B) 206 (1998) 583.
[9] V.V. Killedar, C.D. Lokhande, C.H. Bhosale, Thin Solid Films 289 (1996) 14.
[10] N.S. Yesugade, C.D. Lokhande, C.H. Bhosale, Thin Solid Films 263 (1995) 145.
[11] N. Parhi, B.B. Nayak, B.S. Acharya, Thin Solid Films 254 (1995) 47.
[12] C.D. Lokhande, Mater. Chem. Phys. 27 (1991) 1.
[13] A. Eychmüller, J. Phys. Chem. B 104 (2000) 6514.
[14] T. Trindade, P. O'Brien, N.L. Pickett, Chem. Mater. 13 (2001) 3843.
[15] B. Pejova, I. Grozdanov, submitted for publication.
[16] B. Pejova, A. Tanusevski, I. Grozdanov, J. Solid State Chem. 172 (2003) 381.
[17] B. Pejova, A. Tanusevski, I. Grozdanov, J. Solid State Chem. 174 (2003) 276.
[18] B. Pejova, I. Grozdanov, Mater. Lett. 58 (2004) 666.
[19] B. Pejova, A. Tanusevski, I. Grozdanov, J. Solid State Chem. 177 (2004) 4785.
[20] B. Pejova, I. Grozdanov, Mater. Chem. Phys. 90 (2005) 35.
[21] B. Pejova, I. Grozdanov, Thin Solid Films 408 (2002) 6.
[22] B. Pejova, I. Grozdanov, J. Solid State Chem. 158 (2001) 49.
[23] B. Pejova, I. Grozdanov, Appl. Surf. Sci. 177 (2001) 152.
[24] B. Pejova, M. Najdoski, I. Grozdanov, S.K. Dey, Mater. Lett. 45 (2000) 2694.
[25] B. Pejova, M. Najdoski, I. Grozdanov, S.K. Dey, J. Mater. Chem. 9 (1999) 2889.
[26] R.H. Bube, Photoconductivity of Solids, Krieger Publ. Co., New York, 1978.
[27] T.W. Case, Phys. Rev. 9 (1917) 305.
[28] M.T.S. Nair, P.K. Nair, Semicond. Sci. Technol. 5 (1990) 1225.
[29] I. Grozdanov, M. Ristov, Gj. Sinadinovski, M. Mitreski, Chemtronics 5 (1991) 71.
[30] W. Hofmann, Z. Kristallogr. 86 (1933) 225.
[31] S. Gorer, G. Hodes, J. Phys. Chem. 98 (1994) 5338.
[32] S.M. Sze, Semiconductor Devices, Physics and Technology, Wiley, New York, 1985.
[33] R. Dalven, Introduction to Applied Solid State Physics, Plenum Press, New York, 1990.
[34] K. Seeger, Semiconductor Physics, Springer, Berlin, Wien, New York, 1973.
[35] P.Y. Yu, M. Cardona, Fundamentals of Semiconductors, Springer, New York, 1999.
[36] S.M. Ryvkin, Photoconductivity Effects in Semiconductors, Consultants Bureau, New York, 1964.
[37] M. Green, R.E. Miles, J. Phys. D 6 (1973) L45.
[38] N.W. Aschroft, N.D. Mermin, Solid State Physics, Holt, Rinehart and Winston, New York, 1976.
[39] R.H. Bube, Photoconductivity of Solids, Wiley, New York, 1960.
[40] D.P. Padiyan, A. Marikani, K.R. Murali, Mater. Chem. Phys. 78 (2002) 51.
[41] A.F. Qasrawi, N.M. Gasanly, Phys. Status Solidi A 194 (2002) 81.
[42] D.P. Padiyan, S.J. Ethilton, R. Murugesan, Phys. Status Solidi A 185 (2001) 231.
[43] A.E. Rakhshani, J. Phys.: Condens. Matter 12 (2000) 4391.
[44] M.A. Osman, Physica B 275 (2000) 351.
[45] L.V.A. Calvi, M.H. Taquecita, B.A.V. Vega, J. Phys.: Condens. Matter 11 (1999) 425.
[46] S. Jain, S. Gautam, D.K. Shukla, N. Goyal, Appl. Surf. Sci. 147 (1999) 19.
[47] G. Mathew, J. Philip, J. Phys.: Condens. Matter 11 (1999) 5283.
[48] E. Shatkovskis, J. Vercinski, J. Jagminas, Phys. Status Solidi A 165 (1998) 231.
[49] G. Mathew, K.N. Madhusoodanan, J. Philip, Phys. Status Solidi A 168 (1998) 239.
[50] P. Gupta, S. Chaudhuri, A.K. Pal, J. Phys. D 26 (1993) 1709.
[51] T.P. Chen, T.C. Lee, S. Fung, C.D. Beling, Semicond. Sci. Technol. 8 (1993) 2085.
[52] P.J. Bishop, M.E. Daniels, B.K. Ridley, E.G. Scott, G.J. Davies, Semicond. Sci. Technol. 4 (1989) 639.
[53] S.K. Datta, A.K. Chaudhuri, Semicond. Sci. Technol. 4 (1989) 376.
[54] P.K. Nair, J. Campos, M.T.S. Nair, Semicond. Sci. Technol. 3 (1988) 134.
[55] G.M. von Staszewski, Semicond. Sci. Technol. 3 (1988) 988.
[56] G.I. Kim, J. Shirafuji, Y. Inuishi, J. Phys. C 15 (1982) 3431.
[57] A.S. Siddiqui, J. Phys. C 14 (1981) L699.
[58] M. Hammam, G.J. Adrianssens, W. Grevendonk, J. Phys. C 18 (1985) 2151.